Modified porphyrin–brucine conjugated to gold nanoparticles and their application in photodynamic therapy

Kamil Záruba,[a] Jarmila Králová,[b] Pavel Řezanka,[a] Pavla Poučková,[c] Lenka Veverková[a] and Vladimír Král*[a,d]

Received 12th February 2010, Accepted 5th May 2010
First published as an Advance Article on the web 20th May 2010
DOI: 10.1039/c002823a

Two porphyrin–brucine quaternary ammonium salts were immobilized on gold nanoparticles and their suitability for both *in vitro* and *in vivo* photodynamic therapy (PDT) was assayed using the basaloid squamous cell carcinoma PE/CA-PJ34 cell line. *In vitro* PDT experiments revealed that the gold nanoparticle-bound conjugates were less effective than unbound conjugates in killing cells. However, the same conjugates were more effective in reducing tumor size *in vivo*, with complete tumor regression observed.

Introduction

In the last decade, numerous reviews have described the principle of photodynamic therapy (PDT) in cancer.[1–3] In brief, PDT combines the use of light and chemical compounds, called photosensitizers (PS) to irreversibly damage cancer cells *via* oxidative stress. After absorption of light, the excited PS generate cytotoxic oxygen-based species (singlet molecular oxygen ($^1\Delta_g$), free radicals of O_2^- and OH^-, *etc.*). PS possess numerous properties that make them desirable for use in cancer therapy including: stable composition, low-toxicity in the absence of light, absorbance in the red spectral region, high extinction coefficient, target specificity, and fast elimination from the body.[4]

Contemporary PS drugs include the porphyrins, chlorins, phthalocyanines, phenothiazinium compounds and texaphyrins.[2,5] Most are hydrophobic and aggregate in aqueous media, decreasing their effectiveness for PDT as their ability to generate singlet molecular oxygen is perturbed. Generally, two approaches are used to overcome this reduction in singlet oxygen formation. First, the PS are prepared with polar pendant groups such as pendant amino acids,[6] glycols[7] or thioglycosylated porphyrins.[8] Accordingly, our laboratory has synthesized porphyrin conjugates with glycol,[9] bile acid[10] and cyclodextrins,[11] and their *in vitro* and *in vivo* PDT activity tested. It was shown that these porphyrin conjugates are taken up preferentially by tumor cells and have the potential to be used for PDT to selectively ablate tumors.[9–11]

The second method for overcoming aggregation is to transport the PS in a polar environment by using carriers that either occur naturally in the extracellular environment, such as low-density lipoproteins, and/or artificial nanoparticles. According to contemporary classification, nanoparticles can be divided into two main groups, passive or active depending on their role in PDT.[12] Passive nanoparticles do not influence the PDT activity of the PS. Generally, the PS is either immobilized on the surface or inside the passive nanoparticle. Examples include, biodegradable polyester[13] and non-biodegradable particles like silica,[14] gold,[15] iron oxide and polyacrylamide. As the name suggests, active nanoparticles are involved in PDT by absorbing light and transferring energy to the PS molecule. Active nanoparticles are comprise of quantum dots,[16] self-illuminating[17] and upconverting[18] nanoparticles.

Given that gold nanoparticles are inert,[20] non-biodegradable particles that are easy to prepare and chemically modify[19] and possess desirable photophysical properties,[21] they are ideal for use in nanomedicine. Additionally, it is possible to modify the gold nanoparticles either covalently or noncovalently with PS. Gold nanoparticles modified with the mercapto-derivative of polyethylene glycol behave like unimolecular micelles that contain a hydrophilic exterior and a hydrophobic interior that can be loaded with hydrophopic PS.[22–24] Gold nanoparticles carrying covalently linked drugs on their surface have also been prepared.[25] PS with pendant mercaptoalkyl chains were assayed for reactive oxygen species generation and the PDT efficiency of the nanoparticle conjugates was found to be twice that obtained using the free derivative.[15,23] Gold nanoparticles are also useful in cancer therapy as they possess favourable photothermal properties.[26] The particles can be conjugated with antibodies that are used to track the efficiency with which cancer cells are destroyed by the photothermal gold nanoparticles. For this purpose, gold nanorods absorbing light at near-infrared wavelengths (650–900 nm) were prepared.[27] The combined activity of photothermal nanoparticles with PS-mediated PDT was demonstrated using a cholinium–purpurin conjugate immobilized on gold nanoparticles.[28]

In this study, we used two porphyrin–brucine conjugates (**1**, **2**) that were prepared by *N*-alkylation of the alkaloid brucine with alkylbromotetraphenylporphyrin derivatives (Fig. 1).[29] These conjugates differ only by the tetraphenylporphyrin substitution. **1** (*para*-) and **2** (*meta*-) derivatives have previously been reported for their selective ATP recognition[30] and gel formation,[29] but have yet to be studied for PDT activity. The influence that small variations in structure have on the ability of molecules to

[a]*Department of Analytical Chemistry, Faculty of Chemical Engineering, Institute of Chemical Technology Prague, Technická 5, 166 28 Prague 6. E-mail: kamil.zaruba@vscht.cz, pavel.rezanka@vscht.cz, lenka.veverkova@vscht.cz; Fax: +420-220-444-058*
[b]*Institute of Molecular Genetics, Academy of Sciences of the Czech Republic, Vídeňská 1083, 142 20 Prague 4, Czech Republic. E-mail: kralova@img.cas.cz; Fax: +420-241-063-586*
[c]*First Faculty of Medicine, Charles University in Prague, Kateřinská 32, 121 08, Prague 2, Czech Republic. E-mail: pouckova@volny.cz*
[d]*Zentiva Development (Part of sanofi-aventis Group), U Kabelovny 130, 10237Prague 10, Czech Republic. E-mail: vladimir.kral@vscht.cz; Fax: +420-220-444-058*

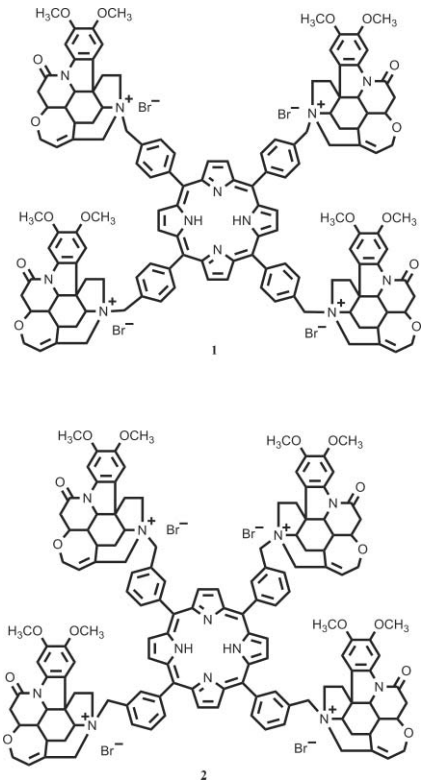

Fig. 1 The structure of **1** and **2**.

interact with solvents,[29] biologically important phosphates[30] and various inorganic anions[31] has already been demonstrated. Here, we present the results of **1** and **2** immobilized on gold nanoparticles and their effectiveness in PDT compared to unbound conjugates.

Results and discussion

Modification by gold nanoparticles

Gold nanoparticles (14.7 nm) prepared by citrate reduction of potassium tetrachloroaurate(III) (**Au-citr**) were modified with 3-mercaptopropanoic acid, and the derivatives **1** and **2** were immobilized. Gold nanoparticles modified with **1** and **2** are labeled **Au-1** and **Au-2**, respectively.

Fluorescence spectra

The fluorescence intensity of **1** and **2** was strongly dependent on the solvent used. The influence of additional compounds on the intensity of emitted fluorescence wavelengths was tested by measuring the emission spectra (excitation of the first Q-band of porphyrins at 520 nm) of **1** and **2** in water, an inorganic salt solution (corresponding to the cell culture media) and a 50 mg mL^{-1} solution of human serum albumin (HSA) (Fig. 2A). In comparison to water, the emission bands of **1** and **2** measured in media were red-shifted (for **1**, from 638 and 700 nm to 644 and 709 nm, and for **2**, from 643 and 707 nm to 647 and 710 nm) and the fluorescence intensity of **1** increased slightly whilst **2** decreased. After immobilizing the porphyrin conjugates on nanoparticles, the intensity of fluorescence emission spectra significantly decreased (Fig. 2B) despite the concentration of porphyrins remaining the same. The weak quantum yield may be

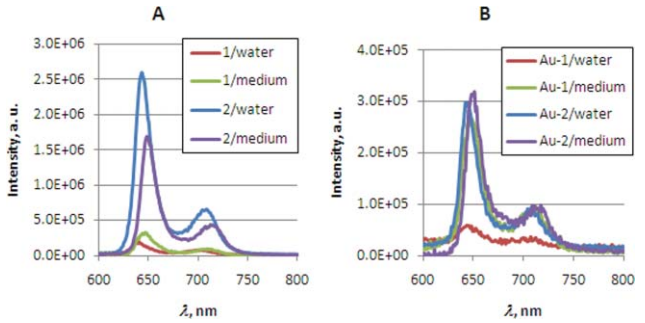

Fig. 2 The fluorescence emission spectra of porphyrins **1** and **2** (left) and porphyrin-modified nanoparticles **Au-1** and **Au-2** (right), in water and cell culture media. Excitation was performed at 520 nm. Porphyrin–brucine conjugates were used at a concentration of 3.5 μM. The concentration of human serum albumin used in growth medium was 50 mg mL^{-1}.

attributed to: (1) both porphyrins and nanoparticles absorbing light at approximately 520 nm, (2) the molecule-to-metal surface energy transfer quenches fluorescence and (3) the modified nanoparticles may partially aggregate. In the case of **Au-1**, aggregation seems to be the cause (Fig. 2B, compare traces "Au-1/water" and "Au-1/medium"), as the intensity of emitted fluorescence was several times higher in cell culture medium compared to water only. These results demonstrate that both *para*- (**1**) and *meta*- (**2**) derivatives aggregate in a solution-dependent manner that is not affected by the presence of PS or immobilization on gold nanoparticles. Importantly, the presence of model plasma proteins present in cell medium dramatically reduced the aggregation of modified nanoparticles. This observation led us to further test these compounds for *in vivo* PDT efficacy.

Intracellular localization

The porphyrin–brucine conjugates (**1** and **2**) were next analyzed for tumor cell uptake and intracellular distribution. The mammary carcinoma cell line, 4T1 was cultivated in the presence of the conjugates for 16 h, during which time the cells were well-dispersed and growing mostly as planar sheets, enabling focused images of fluorescence to be recorded. These cells exhibited punctate red fluorescence (Fig. 3). To identify the intracellular compartment where **1** and **2** accumulate, co-staining with the LysoTracker Green fluorescence probe was performed. The merged images revealed that **1** and **2** colocalized to a subset of LysoTracker-stained structures that represent lysosomes. Similar localization was also observed in PE/CA-PJ34 basaloid squamous cell carcinoma cells, a cell line that was predominantly used in our study (data not shown).

Upon addition of gold nanoparticle conjugated **1** and **2** to cell culture media, aggregates formed, which were visible as a reddish precipitate that covered parts of the cell. These were particularly abundant in the case of **Au-1** (Fig. 4).

In vitro phototoxicity

To investigate the photodynamic potential of the free porphyrin–brucine conjugates or those immobilized on gold nanoparticles, we incubated PE/CA-PJ34 cells in the presence of the conjugates for 16 h and subjected them to PDT. In parallel, cells were incubated with porphyrins without illumination to serve as dark

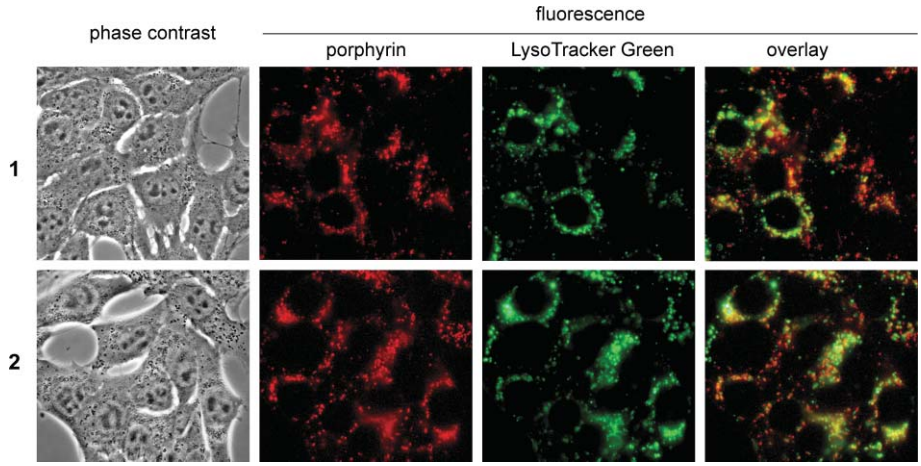

Fig. 3 The intracellular localization of porphyrin–brucine conjugates in 4T1 cells. The middle panels show the red fluorescence of **1** and **2** and co-staining with the lysosomal specific probe (LysoTracker Green); right panels represent an overlay of the green and red images and demonstrate co-localization (shown in orange/yellow). Porphyrin–brucine conjugates were used at a concentration of 2.5 μM.

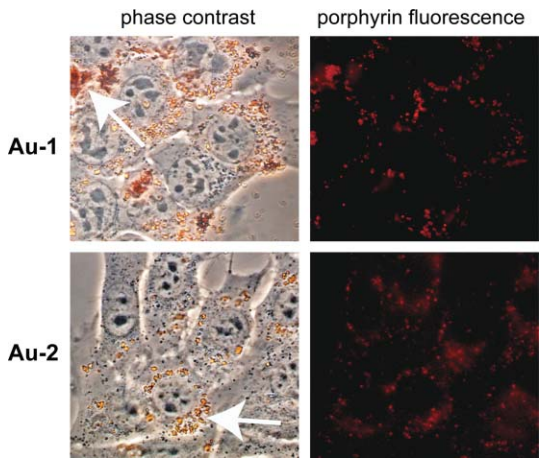

Fig. 4 Difference in aggregation behavior of porphyrin–brucine conjugates immobilized on gold nanoparticles (left panels). 4T1 cells were incubated with **Au-1** and **Au-2** at a concentration of 2.5 μM for 4 h before pictures were taken. Aggregates are highlighted by arrows.

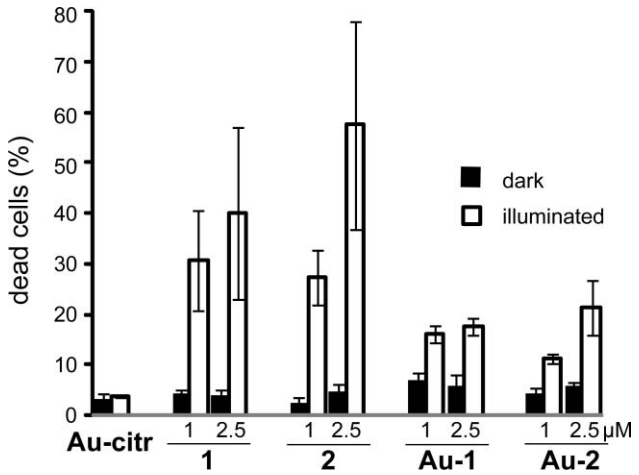

Fig. 5 The effect of free or immobilized porphyrin–brucine conjugates on the induction of cell death *via* PDT. PE/CA-PJ34 cells were incubated with either 1 or 2.5 μM of **1** and **2** or their modified Au-nanoparticles for 16 h. Cells were then illuminated with filtered light (500–520 nm, 7.2 J cm^{-2}). The percentage of dead cells was established the following day by using the Trypan blue exclusion method. The average and standard deviation for three independent experiments are shown.

controls. Twenty four hours following the illumination of cells with filtered light, the mortality of post-PDT cultures were determined (Fig. 5). Satisfyingly, the induction of cell death was both light and drug-dose dependent. Control cells incubated with unconjugated gold nanoparticles (**Au-citr**) did not display any increase in cell death after illumination. Thus, under these *in vitro* conditions we can exclude the possibility that any cell death is due to the photothermal activity of the gold nanoparticles. Interestingly, the phototoxicities of unbound porphyrin–brucine conjugates **1** and **2** were higher than those immobilized on gold nanoparticles. This reduction of photodynamic efficacy is likely to be a consequence of **Au-1** and **Au-2** aggregation that occurs in the aqueous cell growth media (Fig. 4).

In vivo PDT efficacy

Using an *in vivo* mouse cancer model, the PDT effectiveness of the unbound porphyrin–brucine conjugates **1** and **2** was compared with those immobilized on gold nanoparticles (**Au-1**, **Au-2**). Nude mice (NuNu) bearing basaloid squamous cell carcinoma PE/CA-PJ34 cells received by intravenous injection either unmodified porphyrins or their gold nanoparticle-modified counterparts. Six hours post injection, tumors were illuminated with light at a dose of 100 J cm^{-2}. Mice not injected with unmodified porphyrins or nanoparticles served as controls. Tumor size was measured after PDT at regular intervals (Fig. 6). We observed the greatest reduction in tumor growth in mice treated with **Au-1** and **Au-2**. All tumors were eliminated in animals who received these conjugated porphyrins and importantly, no detectable relapse of the primary tumor was observed. In contrast, animals treated with unbound **1** and **2** exhibited only a transient regression in tumor size that lasted until day 18, when the primary tumors began to gradually regrow. Presumably, this relapse in tumor growth is from a small population of tumor cells that survived the PDT. Interestingly,

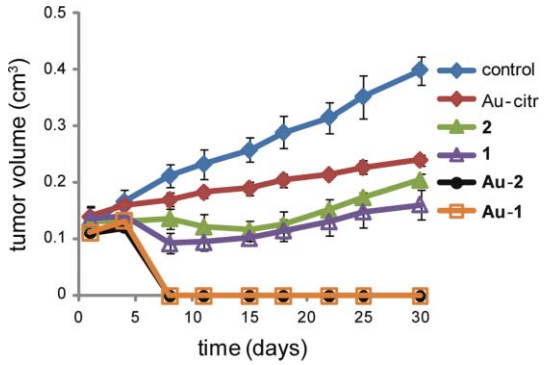

Fig. 6 The PDT effectiveness of **1** and **2** and their respective Au-immobilized nanoparticle counterparts to eradicate mouse tumors. Nude mice (NuNu) bearing subcutaneous PE/CA-PJ34 tumors ($n = 7$ per each group) received an intravenous dose of drug (5 mg kg^{-1}). Tumors were illuminated with light (100 J cm^{-2}) six hours after injection. Tumor size was measured repeatedly and the tumor volume was determined. Control mice were exposed to illumination but did not receive the porphyrin drug. The **Au-citr** group represents mice injected with Au nanoparticles, **1** and **2** groups received porphyrin conjugates, **Au-1** and **Au-2** groups received porphyrin-modified Au nanoparticles.

mice treated with unconjugated gold nanoparticles exhibited a slight tumor retardation in growth that is most likely due to the photo-thermal effect described in other systems.[32–34]

The apparent discrepancy in the *in vitro* and *in vivo* performance of unbound porphyrin–brucine conjugates **1** and **2** and those immobilized on gold nanoparticles (**Au-1** and **Au-2**) is likely to be due to the differing environmental conditions the porphyrin conjugates were exposed to. The fluorescence data revealed that conjugates **1** and **2** were efficiently taken up by cells under the *in vitro* conditions tested. However, in culture media, **Au-1** and **Au-2** tended to aggregate, which resulted in lower intracellular availability (Fig. 4) and PDT efficacy (Fig. 5). Under the *in vivo* conditions tested, the gold nanoparticle-immobilized conjugates were more effective than free conjugates alone. Both spectroscopic and ECD studies demonstrated that conjugated nanoparticles exhibited a strong interaction with plasma proteins (mainly HSA) which led to their self-assembly and the generation of supramolecular complexes. Subsequently, permeability and the retention effect (EPR) were enhanced, resulting in the potent accumulation of **Au-1** and **Au-2** in tumors, which increased their PDT efficacy. Moreover, the direct lethal effect of PDT on tumor cells combines well with the nanoscale size of gold-immobilized porphyrins that may limit the local blood supply (vascular impairment). This hypothesis of vascular damage after PDT with nanoparticles will be the subject of future work.

Conclusions

Our study demonstrates the structure–activity relationship and biological efficacy of low-molecular-weight brucine-functionalized *meso*-tetraphenylporphyrins either unconjugated or immobilized to gold nanoparticles. There is a striking difference in aggregation behaviour depending on the aqueous solution used to resuspend the nanoparticles. Our study revealed that gold nanoparticles may serve as an efficient vector for intra-tumor PS delivery. Thus, the outcome of PDT efficacy for immobilized PS is superior to the classical solution application of PS. In conclusion, compared to free PS, the gold nanoparticle-modified porphyrin derivatives **1** and **2** represent a significant improvement in PDT. The brucine–porphyrin derivatives **1** and **2** bound to modified gold nanoparticles mediate a complete regression of PE/CA-PJ34 carcinoma after photodynamic treatment. These findings demonstrate a new strategy for improving the therapeutic value of PDT.

Experimental section

Preparation of modified gold nanoparticles

Porphyrin–brucine conjugates **1** and **2** were prepared according to the procedure described previously.[29] Gold nanoparticles (14.7 nm) were prepared by citrate reduction of potassium tetrachloroaurate(III) (**Au-citr**). After modification with 3-mercaptopropanoic acid, derivatives **1** and **2** were immobilized as described elsewhere.[33] Here, a solution of **1** or **2** (5 mg) in methanol was added to 50 mL of **Au-citr**. Modified nanoparticles (**Au-1** and **Au-2**, respectively) were isolated by centrifugation after three days of incubation. Using redispersion in methanol, methanol–water, water and dimethylsulfoxide, unbound porphyrin derivatives were removed and **Au-1** and **Au-2** molecules were concentrated to a volume of 1 mL. According to the spectral analysis of supernatants, 0.8 mg of **1** or **2** was present in the final 1 mL solution of **Au-1** and **Au-2** nanoparticles.

Fluorescence measurements

Fluorescence spectra were recorded using a Fluoromax spectrometer (Jobin-Yvon, Japan). A volume of 1 mL of sample was placed into 1 cm plastic cuvettes. The excitation wavelength was 520 nm.

Cell culture and *in vitro* experiments

4T1 (mouse mammary carcinoma) cells were purchased from ATCC and PE/CA-PJ34 (human basaloid squamous cell carcinoma) cells were purchased from ETCC. As described before,[11] all cells were grown exponentially in RPMI 1640 medium with 10% fetal calf serum. For experiments, 1–1.5 × 10^5 cells were seeded into 1.8 cm^{-2} wells and incubated overnight with the porphyrin–brucine conjugates or their counterparts immobilized on gold nanoparticles (1 and 2.5 μM). After incubation, cells were rinsed with PBS, cultured for 1 h in fresh medium without phenol red and illuminated with a 75 W halogen lamp with a band-pass filter (Andover, Salem, NH) that emmitted light at wavelengths between 500–520 nm. The fluence rate at the level of the cell monolayer was 1 mW cm^{-2}, and the total light dose was 7.2 J cm^{-2}. Twenty four hours post irradiation, the viability of PDT-treated cultures was determined by the Trypan blue exclusion method. In parallel, control "dark" experiments (without illumination) were performed.

Microscopic studies

Cells grown on coverslips in 35 mm Petri dishes were incubated with 2.5 μM porphyrin–brucine conjugates in culture medium for 16 h. After washing, porphyrin fluorescence was observed with a DM IRB Leica microscope equipped with a DFC 480 camera

using a ×63 oil immersion objective and Leica filter cube N2.1 (excitation filter BP 515–560 nm and long pass filter LP 590 nm for emission). For labeling lysosomes, 500 nM LysoTracker Green (Molecular Probes) was added to the culture media for 30 min. Cells were washed and examined by fluorescence microscopy using the Leica filter cube I3 (excitation filter BP 450–490 nm and long pass filter LP 515 nm for emission).

In vivo experiments

NuNu mice were subcutaneously injected with basaloid squamous cell carcinoma PE/CA-PJ34 cells as described previously.[11] When the tumor mass reached a volume of 100 mm^3 (10–14 days after injection), mice were intravenously injected with porphyrin–brucine conjugates (5 mg kg^{-1}) resuspended in a volume of 0.1 mL per 20 g mice. Six hours later the tumor area (2 cm^2) was irradiated with a 500–700 nm xenon lamp ONL051 (maximum at 635 nm, Preciosa Crytur, Turnov, Czech Republic) with a total impact energy of 100 J cm^{-2} and fluence rate of 200 mW cm^{-2}. Each experimental group consisted of 7 mice. Tumor size was measured repeatedly and the tumor volume was determined.[11] All aspects of animal experimentation and husbandry were carried out in compliance with national and European regulations and were approved by the institutional committee.

Acknowledgements

This work was funded by the Ministry of Education, Youth and Sports of the Czech Republic (MŠMT6046137307, LC06077), and from the Grant Agency of the Czech Republic (203/09/1311) and from the Academy of Sciences of the Czech Republic (KAN200200651).

Notes and references

1 J. N. Silva, P. Filipe, P. Morliere, J.-C. Maziere, J. P. Freitas, J. L. Cirne, C. de Castro and R. Santus, *Bio-Medical Mater. Engineer.*, 2006, **16**, S147–S154; Y. N. Konan, R. Gurny and E. Allemann, *J. Photochem. Photobiol., B*, 2002, **66**, 89–106; J. S. McCaughan Jr., *Drugs Aging*, 1999, **15**, 49–68.
2 M. R. Detty, S. L. Gibson and S. J. Wagner, *J. Med. Chem.*, 2004, **47**, 3897–3915.
3 B. C. Wilson and M. S. Patterson, *Phys. Med. Biol.*, 2008, **53**, R61–R109.
4 D. Bechet, P. Couleaud, C. Frochot, M.-L. Viriot, F. Guillemin and M. Barberi-Heyob, *Trends Biotechnol.*, 2008, **26**, 612–621.
5 S. B. Brown, E. A. Brown and I. Walker, *Lancet Oncol.*, 2004, **5**, 497–508; A. E. O'Connor, W. M. Gallagher and A. T. Bryne, *Photochem. Photobiol.*, 2009, **85**, 1053–1074.
6 H. M. Wang, J. Q. Jiang, J. H. Xiao, R. L. Gao, F. Y. Lin and X. Y. Liu, *Chem.-Biol. Interact.*, 2008, **172**, 154–158.
7 S. Banfi, E. Caruso, S. Caprioli, L. Mazzagatti, G. Canti, R. Ravizza, M. Gariboldi and E. Monti, *Bioorg. Med. Chem.*, 2004, **12**, 4853–4860; M. Sibrian-Vazquez, T. J. Jensen and M. G. H. Vincente, *J. Photochem. Photobiol., B*, 2007, **86**, 9–21.
8 I. Sylvain, R. Zerrouki, R. Granet, Y. M. Huang, J.-F. Lagorce, M. Guilloton, J.-C. Blais and P. Krausz, *Bioorg. Med. Chem.*, 2002, **10**, 57–69.
9 J. Králová, T. Bříza, I. Moserová, B. Dolenský, P. Vašek, P. Poučková, Z. Kejík, R. Kaplánek, P. Martásek, M. Dvořák and V. Král, *J. Med. Chem.*, 2008, **51**, 5964–5973.
10 J. Králová, J. Koivukorpi, Z. Kejík, P. Poučková, E. Sievänen, E. Kolehmainen and V. Král, *Org. Biomol. Chem.*, 2008, **6**, 1548–1552.
11 J. Králová, A. Synytsya, P. Poučková, M. Koc, M. Dvořák and V. Král, *Photochem. Photobiol.*, 2006, **82**, 432–438.
12 D. K. Chatterjee, L. S. Fong and Y. Zhang, *Adv. Drug Delivery Rev.*, 2008, **60**, 1627–1637.
13 Y. N. Konan, M. Berton, R. Gurny and E. Allemann, *Eur. J. Pharm. Sci.*, 2003, **18**, 241–249; Y. N. Konan, R. Cerny, J. Favet, M. Berton, R. Gurny and E. Allemann, *Eur. J. Pharm. Biopharm.*, 2003, **55**, 115–124.
14 I. Roy, T. Y. Ohulchanskyy, H. E. Pudavar, E. J. Bergey, A. R. Oseroff, J. Morgan, T. J. Dougherty and P. N. Prasad, *J. Am. Chem. Soc.*, 2003, **125**, 7860–7865.
15 M. E. Wieder, D. C. Hone, M. J. Cook, M. M. Handsley, J. Gavrilovic and D. A. Russell, *Photochem. Photobiol. Sci.*, 2006, **5**, 727–734.
16 A. C. Samia, X. Chen and C. Burda, *J. Am. Chem. Soc.*, 2003, **125**, 15736–15737.
17 W. Chen and J. Zhang, *J. Nanosci. Nanotechnol.*, 2006, **6**, 1159–1166.
18 P. Zhang, W. Steelant, M. Kumar and M. Scholfield, *J. Am. Chem. Soc.*, 2007, **129**, 4526–4527.
19 R. Shenhar and V. M. Rotello, *Acc. Chem. Res.*, 2003, **36**, 549–561; M. Grzelczak, J. Pérez-Juste, P. Mulvaney and L. M. Liz-Marzan, *Chem. Soc. Rev.*, 2008, **37**, 1783–1791.
20 E. E. Connor, J. Mwamuka, A. Gole, C. J. Murphy and M. D. Wyatt, *Small*, 2005, **1**, 325–327.
21 Y. Sun and Y. Xia, *Analyst*, 2003, **128**, 686–691.
22 Y. Cheng, A. C. Samia, J. D. Meyers, I. Panagopoulos, B. Fei and C. Burda, *J. Am. Chem. Soc.*, 2008, **130**, 10643–10647.
23 Y. Cheng, A. C. Samia, J. Li, M. E. Kenney, A. Resnick and C. Burda, *Langmuir*, 2010, **26**, 2248–2255.
24 C. K. Kim, P. Ghosh, C. Pagliuca, Z.-J. Zhu, S. Menichetti and V. M. Rotello, *J. Am. Chem. Soc.*, 2009, **131**, 1360–1361.
25 R. A. Sperling, P. R. Gil, F. Zhang, M. Zanella and W. J. Parak, *Chem. Soc. Rev.*, 2008, **37**, 1896–1908.
26 V. P. Zharov and V. Galitovsky, *Appl. Phys. Lett.*, 2003, **83**, 4897–4899.
27 I. H. El-Sayed, X. Huang and M. A. El-Sayed, *Cancer Lett.*, 2006, **239**, 129–135; X. Huang, I. H. El-Sayed, W. Qian and M. A. El-Sayed, *J. Am. Chem. Soc.*, 2006, **128**, 2115–2120; X. Huang, P. K. Jain, I. H. El-Sayed and M. A. El-Sayed, *Photochem. Photobiol.*, 2006, **82**, 412–417.
28 D. Demberelnyamba, M. Ariunaa and Y. K. Shim, *Int. J. Mol. Sci.*, 2008, **9**, 864–871.
29 V. Král, S. Pataridis, V. Setnička, K. Záruba, M. Urbanová and K. Volka, *Tetrahedron*, 2005, **61**, 5499–5506.
30 Z. Kejík, K. Záruba, D. Michalík, J. Šebek, J. Dian, S. Pataridis, K. Volka and V. Král, *Chem. Commun.*, 2006, 1533–1535.
31 L. Veverková, K. Záruba, J. Koukolová and V. Král, *New J. Chem.*, 2010, **34**, 117–122.
32 D. P. O'Neal, L. R. Hirsch, N. J. Halas, J. D. Payne and J. L. West, *Cancer Lett.*, 2004, **209**, 171–176.
33 P. Řezanka, K. Záruba and V. Král, *Tetrahedron Lett.*, 2008, **49**, 6448–6453.
34 N. F. Gamaleia, E. D. Shishko, G. A. Dolinsky, A. B. Shcherbakov, A. V. Usatenko and V. V. Kholin, *Exp. Oncol.*, 2010, **32**, 44–47. During the revision of our manuscript, an article by Gamaleia *et al.* that describes the *in vitro* PDT activity of hematoporphyrin–gold nanocomposites was published. Interestingly, the authors utilized transformed cell lines to demonstrate much higher PDT activities with conjugates than that of the original PS. However, missing *in vivo* data and the use of different sensitizers and cell lines make the direct comparison with our study impossible.

